ARMY RESEARCH LABORATORY

Monte Carlo Evaluation of Tritium Beta Spectrum Energy Deposition in Gallium Nitride (GaN) Direct Energy Conversion Devices

by Marc Litz

ARL-TR-7082 **September 2014**

NOTICES

Disclaimers

The findings in this report are not to be construed as an official Department of the Army position unless so designated by other authorized documents.

Citation of manufacturer's or trade names does not constitute an official endorsement or approval of the use thereof.

Destroy this report when it is no longer needed. Do not return it to the originator.

Army Research Laboratory
Adelphi, MD 20783-1138

ARL-TR-7082 **September 2014**

Monte Carlo Evaluation of Tritium Beta Spectrum Energy Deposition in Gallium Nitride (GaN) Direct Energy Conversion Devices

Marc Litz
Sensors and Electron Devices Directorate, ARL

REPORT DOCUMENTATION PAGE

Form Approved
OMB No. 0704-0188

1. REPORT DATE *(DD-MM-YYYY)*	2. REPORT TYPE	3. DATES COVERED (From - To)
September 2014	Final	January–July 2014

4. TITLE AND SUBTITLE
Monte Carlo Evaluation of Tritium Beta Spectrum Energy Deposition in Gallium Nitride (GaN) Direct Energy Conversion Devices

5a. CONTRACT NUMBER

5b. GRANT NUMBER

5c. PROGRAM ELEMENT NUMBER

6. AUTHOR(S)
Marc Litz

5d. PROJECT NUMBER

5e. TASK NUMBER

5f. WORK UNIT NUMBER

7. PERFORMING ORGANIZATION NAME(S) AND ADDRESS(ES)
U.S. Army Research Laboratory
ATTN: RDRL-SED-E
2800 Powder Mill Road
Adelphi, MD 20783-1138

8. PERFORMING ORGANIZATION REPORT NUMBER
ARL-TR-7082

9. SPONSORING/MONITORING AGENCY NAME(S) AND ADDRESS(ES)

10. SPONSOR/MONITOR'S ACRONYM(S)

11. SPONSOR/MONITOR'S REPORT NUMBER(S)

12. DISTRIBUTION/AVAILABILITY STATEMENT
Approved for public release; distribution unlimited.

13. SUPPLEMENTARY NOTES

14. ABSTRACT
In this report, a Monte Carlo nuclear scattering code—Monte Carlo n-particle extended (MCNPX)—was used to investigate the possibility of using gallium nitride (GaN) semiconductors for the purpose of converting the low energy β emitted during natural decay of tritium (^{3}H) into electrical current for use in a power source. The shape of the beta decay spectrum differs in isotopes because of screening potentials and forbidden transitions. Therefore the use of average energy or endpoint energy is not sufficient for a detailed understanding of energy deposition in a material. The technique of direct energy conversion (DEC) is considered advantageous with GaN compared to that of silicon carbide (SiC). GaN has a direct band gap material of 3.4 eV compared to the more commonly used SiC with a 3.2-eV indirect band gap. The beta emission spectrum from ^{3}H, directed toward a GaN converter is modeled. A GaN device optimized to stop all β in ^{3}H would be less than 1.5 μm thick. The depletion region in a GaN DEC that would enclose 99% of the charge generated by separated electron hole pairs is calculated to be 700 nm thick for ^{3}H.

15. SUBJECT TERMS
isotope battery, direct energy conversion, tritium, Monte Carlo, MCNPX

16. SECURITY CLASSIFICATION OF:			17. LIMITATION OF ABSTRACT	18. NUMBER OF PAGES	19a. NAME OF RESPONSIBLE PERSON
a. REPORT	b. ABSTRACT	c. THIS PAGE			Marc Litz
Unclassified	Unclassified	Unclassified	UU	22	19b. TELEPHONE NUMBER (*Include area code*) 301-394-5556

Contents

List of Figures iv

List of Tables iv

1. Introduction 1

2. Problem Geometry 1

3. Results 3

3.1 Electron Flux in GaN 3

3.2 Evaluation of Free Carriers 4

3.3 Electron Energy Deposition in GaN....5

3.4 Comparison of Electron Range 7

4. Conclusions 7

5. References 9

Appendix. MCNPX Input Deck 11

List of Symbols, Abbreviations, and Acronyms 14

Distribution List 15

List of Figures

Fig. 1 The intensity of β-emission spectrum of ^{3}H shows that the largest β-flux is at 2.5 keV (12.5% of the flux) 2

Fig. 2 Side view of a cylindrical geometry composed of GaN p-i-n fabricated for initial energy conversion evaluations 2

Fig. 3 Flux of electrons (per incident decay beta) generated in GaN as a function of depth in the material. The flux drops by a factor of 5000 front to back. b) Spectrum of electron energy as a function of depth in GaN is similar to ^{3}H decay spectrum. The maximum electron energy decreases from 18.6 keV in the top layer to 11 keV in the eighth layer (1600 nm). 3

Fig. 4 Number of EHPs created from one incident electron as a function of energy is shown compared to the number of EHPs calculated from 100 mCi of the tritium weighted spectrum 5

Fig. 5 a) Cross-sectional image of electron energy deposition inside the GaN DEC. b) Electron energy deposition is integrated along the depth. 68% of the energy is deposited in 150 nm. 6

List of Tables

Table 1 CSDA electron range in GaN for three commonly available isotopes 7

1. Introduction

Long-lived power sources offer high potential in applications of power sources for unattended sensors and communications nodes.[1,2] Recent commercial advances have been described with the goal of developing tritium (^{3}H)-powered silicon carbide (SiC) direct energy conversion (DEC) sources generating energy harvesting levels of power.[3,4,9] In a direct band gap material, absorption of light is generally greater because there are fewer competing (losses) mechanisms for energy transfer. Common direct band gap materials include the III-V semiconductors gallium nitride (GaN), gallium arsenide (GaAs), and indium phosphide (InP). Common indirect band materials are silicon (Si), SiC, diamond (C), and germanium (Ge). Therefore, direct band gap materials can be more efficient at elevating valence electrons into the conduction band for photovoltaic applications than indirect band gap materials.

A series of simulation were designed and performed to evaluate the possibility of using GaN as a radiation-tolerant, wide band gap semiconductor. The semiconductor material can convert the kinetic energy of emitted betas in radioactive decay emissions into a series of lower energy electron-hole pairs (EHPs) and knock-on electrons. These secondary electrons are swept away in the electric field of the depletion region in the semiconductor junction and collected, forming current flow in a circuit. The nW/cm^2 power generated is typical of energy harvesting levels of power.[11] Radioisotope power sources differ from typical renewable energy/power levels in that they are continuously on for the lifetime of the isotope decay. The power output degrades by half with each half-life (12.6 years for ^{3}H) of the isotope, so useful energy can be harvested for at least two half-lives (decades).

2. Problem Geometry

The simulations model a volume of gas emitting a beta spectrum from ^{3}H. The maximum energy emitted from the decay of ^{3}H is 18.6 keV. The decay reaction ${}^3H \Rightarrow {}^3He + \beta + \nu$ creates a helium, beta, and anti-neutrino. The final beta spectrum from ^{3}H is shown in Fig. 1. 12.5% of the emitted betas have 2.5 keV energy. The average β-energy is 5.7 keV. A sample GaN p-i-n device was fabricated by metallo-organic chemical vapor deposition (MOCVD) at the State University of New York (SUNY). The sample, illustrated in Fig. 2, was modeled using the Monte Carlo n-particle extended (MCNPX) nuclear scattering code.[10] MCNPX is a general-purpose Monte Carlo code that can be used to model neutron, photon, and electron (or coupled) transport. The code uses an extensive collection of cross-sectional data and is able to simulate the transportation of these particles with energy from 1 keV to 100 MeV in materials.

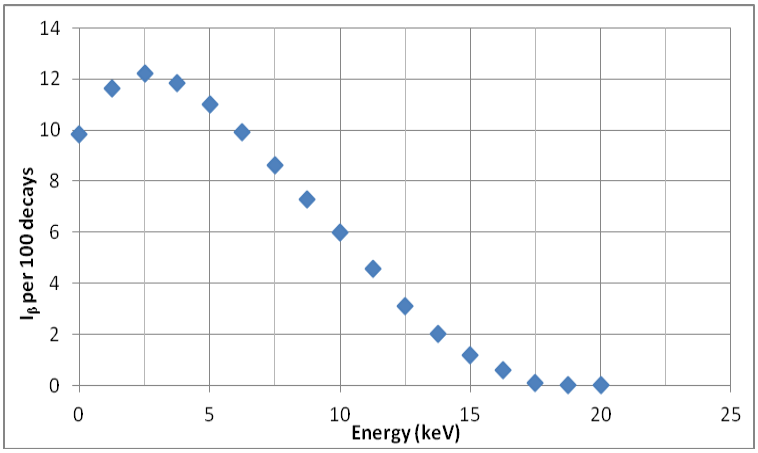

Fig. 1 The intensity of β-emission spectrum of ^{3}H shows that the largest β-flux is at 2.5 keV (12.5% of the flux)

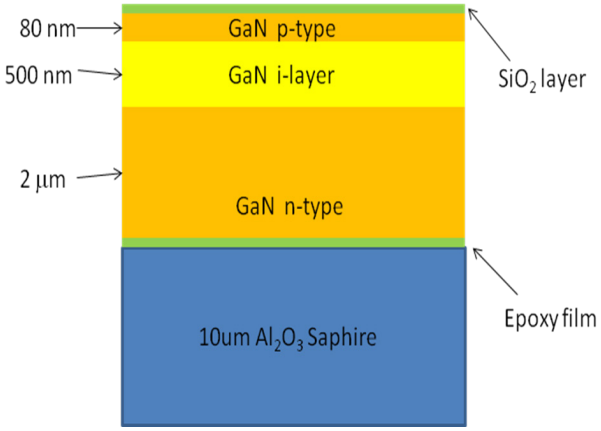

Fig. 2 Side view of a cylindrical geometry composed of GaN p-i-n fabricated for initial energy conversion evaluations

As mentioned, the ^{3}H beta emission spectrum is shown in Fig. 1.[5,12] The shape of the beta spectrum differs in isotopes because of screening potentials and forbidden transitions. Therefore, using average energy or endpoint energy is not sufficient for a detailed understanding of energy deposition in a material. The shape of the beta emission spectrum is responsible for variation in energy deposition as a function of depth in materials. The ^{3}H energy spectrum is defined in the source definition section of the MCNPX input deck detailed in the Appendix.

The energy emitted in a decay of ^{3}H is 18.6 eV. One electron is emitted in each decay of the ^{3}H isotope. The β spectral intensity I_{β} shows that 12.5% of the betas are ~2.5 keV. The median energy is 6.1 keV. The β spectrum of Fig. 1 is used as input for the MCNPX calculation, as described in the source definition section of the Appendix.

3. Results

The electron flux is calculated in MCNPX, and then compared to a model of EHP creation efficiency and electron beam induced current (EBIC) measurements in semiconductors. The expected values of number of EHPs created in each case are compared.

3.1 Electron Flux in GaN

The electron flux/cm^2 was calculated in 200-nm increments throughout the depth of the GaN cylindrical volume, which extends from 0–2.58 μm along the axis of the cylinder (Fig. 3a). The graph of electron flux throughout the depth of the material shows charge accumulation along the surfaces (both top and bottom). The β-spectrum in each of the eight 200-nm layers is shown in Fig. 3b. The spectrum in the top (first) 200-nm layer shows energy content out to 18.6 keV as expected in the full ^{3}H emission spectrum. The β-spectrum at the bottom end of the GaN volume is limited to 11 keV maximum content. The flux at the bottom of the GaN device is 10^{-5} times reduced (2.58 μm thick).

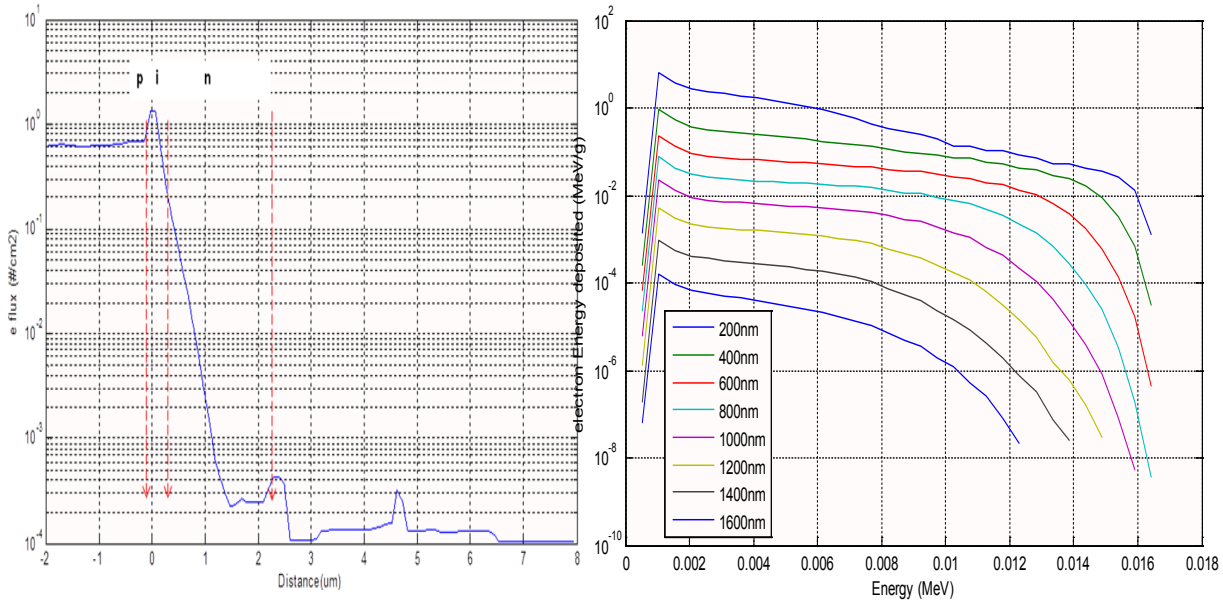

a) b)

Fig. 3 Flux of electrons (per incident decay beta) generated in GaN as a function of depth in the material. The flux drops by a factor of 5000 front to back. b) Spectrum of electron energy as a function of depth in GaN is similar to ^{3}H decay spectrum. The maximum electron energy decreases from 18.6 keV in the top layer to 11 keV in the eighth layer (1600 nm).

The existing ^{3}H power sources purchased from mb-microtec Inc provide 120 mCi/cm^2 from the rectangular parallelepiped ^{3}H -filled vials. The β-flux resulting is 4.4x10^9 β/cm^2*s. This corresponds to a current density of 4.4 nA/cm^2. The initial nuclear power, P_{nuc}, from decay β emitted (5.7 keV E_{avg}) is then 4μW/cm^2.

3.2 Evaluation of Free Carriers

The analysis of Klein describes the energy consumed in the creation of an EHP (ε_{ehp}). The energy required to generate an EHP is understood to include three loss mechanisms.[8] They include 1) band gap energy (E_g), 2) thermalization loss or residual kinetic energy of electrons with insufficient energy to reach conduction band, and 3) phonon losses (lattice vibrations, *r*).

$$\varepsilon_{ehp} = (1+\frac{9}{5})E_g * r(\hbar\omega_r), \quad (1)$$

where ε_{ehp} is the energy consumed in creation of an EHP and r represents the phonon losses (Raman quanta emitted by ionization impact). The 9/5 factor in Eq. 1 is experimentally determined as useful to describe thermalization losses.

The band gap of GaN (3.4 eV) is small compared to the E_{avg} of incident β decay of 5700 eV. The excess energy available per incident β could create a maximum of (5700/3.4) 1676 secondary electrons if no energy was lost in the process. However, the phonon and thermal losses reduce the efficiency of secondary creation to 30% in GaN. This is equivalent to requiring ~10eV from each incident β to create an EHP instead of just the band gap energy of 3.4 eV. Therefore, the number of secondaries created could be as many as 570 per each incident β of average energy 5700 eV. Given that the β flux calculated for 100 mCi/cm^2 ^{3}H vials of 4.4x10^9 β/cm^2*s, then we might expect as many as 2.5x10^{12} β/cm^2*s within the volume of the intrinsic region of the GaN converter or 400 nA/cm^2. How well we can collect these free charges from the device is another question.

The number of EHPs generated in the EBIC diagnostic technique is

$$Nehp = \frac{E}{3.2E_g}(1-\frac{\alpha E_{bs}}{E}), \quad (2)$$

where E is the energy of the incident electron, E_g the energy gap, E_{bs} the mean energy of backscattered electrons, and α the backscattering coefficient.[7] The measured values for number of EHPs created in the EBIC diagnostic technique has been experimentally quantified in Eq. 2. Using typical values for backscatter energy of 10% of incoming β energy and a backscatter coefficient of 1, we can calculate an upper limit for the number of EHPs expected as a function of incoming β energy. The result is shown in the top curve of Fig. 4. The second curve in Fig. 4 is calculated using the weighted number spectrum of ^{3}H emission from 100 mCi/cm^2. By this approach, as many as 4.4x10^{12} free electrons (area under curve) could be available for collection, possibly generating as much as 750 nA/cm^2.

The analysis of Bresse[7] accounts for the number of EHPs created from incoming electrons while the analysis of Klein[8] focuses on the mechanisms of loss in creation of EHPs. Both methods offer an upper bound of free carriers in the device. Experimental measurement of EBIC techniques can generate as much as 750 nA/cm^2 in free carriers that could be harvested for potential use in a GaN DEC device. By calculating the energy lost in the creation of an individual EHP, as much as 400 nA/cm^2 could be generated. These expected values are at least in the same order of magnitude.

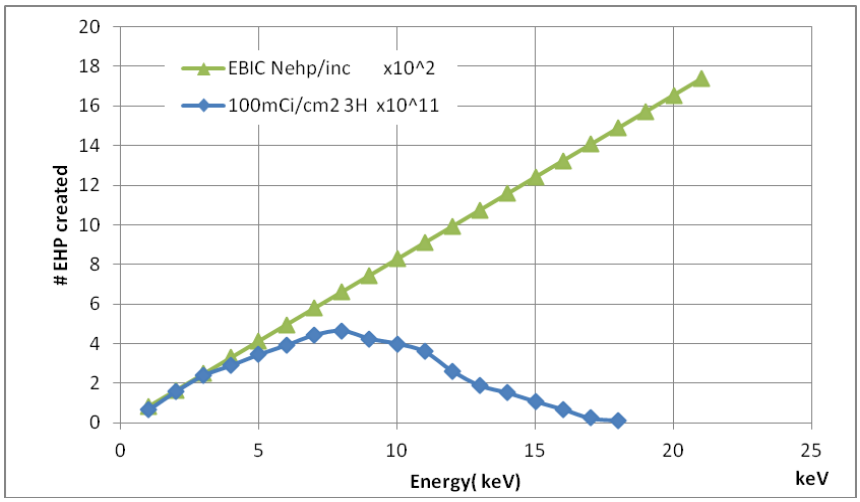

Fig. 4 Number of EHPs created from one incident electron as a function of energy is shown compared to the number of EHPs calculated from 100 mCi of the tritium weighted spectrum

3.3 Electron Energy Deposition in GaN

In answer to the question of how big should one design the i-layer in order to maximize maximum charge collection efficiency, the MCNPX simulation numerical result of energy deposition in the material provides guidance. The MCNPX simulation models nuclear scattering, not electron transport in fields. Therefore, n- and p-doping differentiation is not significant in these calculations. The top of the cylindrical GaN structure is uniformly illuminated over the entire surface with the β emission spectrum of ^{3}H, as shown in Fig. 2.

The logarithmic contour plot of energy deposited (MeV/g) in the GaN device is shown in Fig. 5a. The mass of a 200-nm-thick, 1-cm-diameter GaN layer is 96 µg. Eight 200-nm layers are included in this model. The two dimensional (2-D) image (Fig. 5a) should be compared to the illustrated line drawing of the device in Fig. 1. The energy deposited is integrated over distance in Fig. 5b. We see that 68% of the energy is deposited in 150 nm and 99% of the energy is deposited in 700 nm.

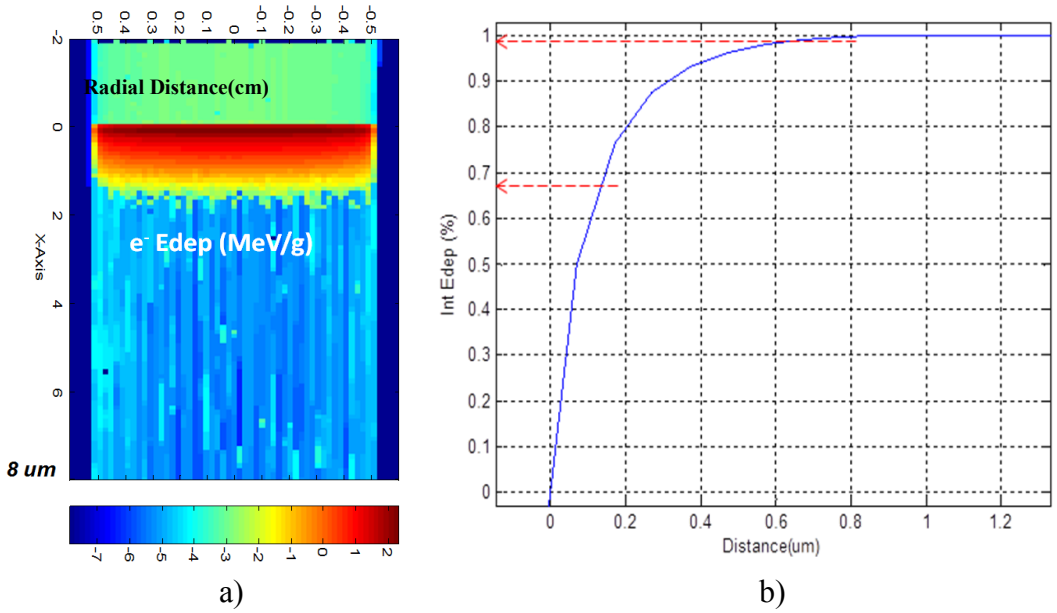

Fig. 5 a) Cross-sectional image of electron energy deposition inside the GaN DEC. b) Electron energy deposition is integrated along the depth. 68% of the energy is deposited in 150 nm.

Corroborating results are always useful to track when using large simulation codes in order to confirm that the correct physics models were chosen for the code. Gallium characteristic x-rays result in the photon energy spectrum. They are observed at the K-alpha and K-beta lines of 9,251.74 and 9,224.82, respectively.[6] These low energy x-rays do not contribute in a significant way to any radiation dose, as only 81 of 100M electrons contribute to the fluorescent lines. The simulation also predicts that 0.5% of the incident β contributes to a bremsstrahlung production spectrum, also an insignificant dose level. These numbers are small compared to 24.2% knock-on electrons generated. The current generated in the GaN device from knock-ons (electron-electron scattering) is expected to be $1x10^9$ e^-/cm^2 or ~160 pA.

The statistical figure of merit (FOM) common to all results in the simulations is proportional to the square of the signal-to-noise ratio (SNR).[2] The FOM is recorded for each signal or spectrum tally. The standard deviation of each numerically calculated result is determined.

$$FOM = \frac{x_n}{\sigma^2 t} = \frac{1}{t\sqrt{N}} \sqrt{\frac{\overline{x^2} - x_n^{\,2}}{x_n^{\,2}}} \tag{3}$$

As can be seen from Eq. 3, the FOM is inversely proportional to t, the time it takes to run the simulation, which is directly proportional to the number of histories calculated. The standard deviation, σ, measures the uncertainty related to statistical fluctuations. It does not quantify the accuracy (or truth) as it relates to the physical quantity.

3.4 Comparison of Electron Range

The MCNPX calculation described in Section 3.3 provides more detail than using the continuously slowing down approximation (CSDA) that was formalized and tabulated into National Institute of Standards and Technology (NIST) reference tables.[14] The three energies of significance in a β-spectrum that describe the spectrum shape are the maximum energy, average energy, and energy with the highest flux intensity. For ^{3}H, those energies are 18.6, 5.7, and 2.5 keV, respectively. The CSDA range in GaN for each energy is shown in Table 1. The range at which 68% and 95% of the free carrier energy is deposited into the GaN for ^{3}H is calculated in the MCNPX simulation, resulting in 0.15 and 0.7 μm, respectively. It is interesting that the CSDA range (0.13 μm) for the most probable electron energy (2.5 keV) is close to the distance for 68% energy deposition (0.15 μm) and the CSDA range (0.7 μm) for average energy (5.7 keV) is equal to the range of 95% energy deposition. The shape of the beta spectrum will impact this correlation, so it is not a generally useful analogy; however, many β spectra do have a similar shape to the ^{3}H (unlike a nickel isotope [^{63}Ni] and promethium isotope [^{147}Pm]).

Table 1 CSDA electron range in GaN for three commonly available isotopes

		NIST		NIST		NIST
	E_{MaxInt}	eRange	E_{avg}	eRange	E_{max}	eRange
	keV	*um*	*keV*	*um*	*keV*	*um*
3H	2.5	0.13	5.7	0.7	18.6	4
63Ni	1	0.03	17.2	4	67	42
147Pm	1	0.03	62	40	224	330

4. Conclusions

^{3}H is the most available and inexpensive of the isotopes mentioned in this report. The modeling result using the full β spectrum of ^{3}H suggests that the i-layer should be between 150–700 nm thick for ^{3}H fuel in order to enclose 68–99% of the generated free carriers. The optimized ranges for ^{63}Ni and ^{147} Pm would be larger because of energies typically 3 and 12 times larger than that of ^{3}H. The optimized depths for these isotopes will be calculated in a future report.

In these calculations, it is seen that the use of energy defined by maximum flux, the average over spectrum, and maximum of ^{3}H beta spectrum can be used as indicators of energy distribution in the material; however, a more detailed Monte Carlo analysis provides a higher degree of accuracy and understanding.

Three approaches to estimating the upper limit of the free carriers created have been described. The energy required (and loss mechanisms) in EHP creation is largely based on the band gap of the semiconductor and phonon losses, and results in a 400 nA/cm^2 estimate. The number of EHPs generated in an EBIC diagnostic technique (based on E_g and energy of incident) suggests a result of 750 nA/cm^2. The number of knock-on electrons generated in the collisions of incident β with GaN atoms is estimated to be ~200 pA. The MCNPX simulation experimentally arrived probability distribution functions and theoretical constructs are meant for 10 keV and above, but have been useful down to 1 keV. Therefore, when using MCNPX to calculate free carriers, a value of 1 keV is definitely to be considered a lower limit, because many inelastic scattering events below 1 keV occur before the 10 eV events begin to have impact on the generation of secondary free carriers.

5. References

1. Eiting CJ, Krishnamoorthy V, Rodgers S, George T, David Robertson J, Brockman John. Demonstration of a radiation resistant, high efficiency SiC betavoltaic. Appl. Phys. Letters. 2006;88:064101.
2. Zhang K, Pathak P, Cerrina F, Ma Z. Performance prediction of nuclear micro power sources based on beta emitters. ECS Transactions. 2009;19(26):45–50.
3. Schroder Dieter K. Progress in SiC materials/devices and their competition. Intl J High Speed Electronics and Systems. 2012;21(1).
4. Clarkson JP, Sun W, Hirschman KD, Gadeken LL, Fauchet PM. Betavoltaic and photovoltaic energy conversion in three-dimensional macroporous silicon diodes. Phys. Stat. Sol. (a). 2007;204:1536–1540.
5. Cross WG, Ing H, Freedman N. A short atlas of beta-ray spectra. Phys. Med. Biol. 1983;28(11):1251–1260.
6. X-Ray Data Booklet, LBNL Pub-490 Rev.3, 2009, Table 1-2. Photon energies, in electron volts, of principal K-, L-, and M-shell emission lines; and JA Bearden, X-Ray Wavelengths. Rev. Mod. Phys. 1967;39:78.
7. Bresse JF. Quantitative investigation in semiconductor devices by electron beam induced current mode: a review. in Scanning Electron Microscopy. 1978;1:717–725. or 1982?IV, 1487–1500 SEM Inc., AMF Ohare Chicago IL.
8. Klein C. Bandgap dependence and related features of radiation ionization energies in semiconductors. J. Appl. Phys. March 1968;39:4.
9. Morkoç H, Strite S, Gao GB, Lin ME, Sverdlov B, Burns M. Large bandgap SiC III-V nitride, and II-VI ZnSe based semiconductor device Technologies. Appl. Phys. Lett. 2005;86:011915.
10. Pelowitz DB. ed. MCNPX user's manual, version 2.7.0. Los Alamos National Laboratory report LA-CP-11-00438, April 2011.
11. Vullers RJM, van Schaijk R, Doms I, Van Hoof C, Mertens R. Micropower energy harvesting. Solid-State Electronics. 2009;53:684–693.
12. Holschuh E. Measurement of the neutrino mass from tritium P-decay. Rep Prog. Phys. 1992;55:1035–1091.

13. Seltzer SM, Berger MJ. Improved procedure for calculating the collision stopping power of elements. Int. J. of Appl. Rad. 1984;35:665.

14. Gumus H. Simple stopping power formula for low and intermediate energy electrons. Radiation Physics and Chemistry. January 2005;72(1):7–12.

Appendix. MCNPX Input Deck

The input deck for the calculation of electron transport in gallium nitride (GaN) is documented below. The file name is GaNDECTr4.txt. The first two sections connect materials to volume geometries. The materials for each volume are defined in the third section. The source stimulus is defined in the fourth section. Type of physics to be included in simulation is defined in the fifth section. Choices of results displayed and tabulated are defined in sixth and seventh sections.

```
Model of GaN-DEC 3H
c ----------------------------------------------------------
c energy deposition modeliing
c +-------------------------------------------------------+
c |                  Cell Cards                           |
c +-------------------------------------------------------+
c # mat   density   surface        data
  3  4    -6.15     -3    imp:e,p 1  u=1    $GaN layer 1
  4  4    -6.15     -4    imp:e,p 1  u=1    $GaN layer 2
  5  4    -6.15     -5    imp:e,p 1  u=1    $GaN  layer 3
  6  4    -6.15     -6    imp:e,p 1  u=1    $GaN  layer 4
  7  4    -6.15     -7    imp:e,p 1  u=1    $GaN  layer 5
  8  4    -6.15     -8    imp:e,p 1  u=1    $GaN  layer 6
  9  4    -6.15     -9    imp:e,p 1  u=1    $GaN 7
 10  4    -6.15     -10   imp:e,p 1  u=1    $GaN 8
 11  9    -3.98     -11   imp:e,p 1  u=1    $Al2O3 1st-layer
 12  1    -.00001     -12   imp:e,p 1  u=1    $Tr vol
c air encasing
 13  2    -0.00129   -13  3 4 5 6 7 8 9 10 11 12 imp:e,p 1  u=1
 14  0 13                      imp:e,p 1  u=1
c room
 15  2    -0.00129   -14       imp:e,p 1 fill=1
 16  0               14       imp:e,p 0        $outside world

c +-------------------------------------------------------+
c |                  Surface Cards                        |
c +-------------------------------------------------------+
c # type param
c 2   rcc  0 -.00001 0   0 0.00001 0  .5     $SiO2 100nm
 3   rcc   0  0.0 0          0 0.00002 0  .5   $GaN p  200nm
 4   rcc   0 0.00002 0   0 0.00002 0  .5   $GaN i
 5   rcc   0 0.00004 0   0 0.00002 0  .5   $GaN n
 6   rcc   0 0.00006 0   0 0.00002 0  .5   $GaN 4
 7   rcc   0 0.00008 0   0 0.00002 0  .5   $GaN n5
 8    rcc  0 0.00010 0   0 0.00002 0  .5   $GaN n6
 9    rcc  0 0.00012 0   0 0.00002 0  .5   $GaN  7
10   rcc  0 0.00014 0   0 0.00002 0  .5   $GaN 8
11   rcc  0 0.00016 0   0 0.00002 0  .5   $Al2O3 3
c source
12   rcc  0 -0.0002 0   0 0.0002 0  0.5   $Tr (2um thick)
c airto encase GaN
13   rpp -1.0 1.0    -.001 .001   -1.1 1.1   $encasing air
c room dimensions
14   rpp -1.2 1.2    -1.2 1.2   -1.2 1.2  $room air

c +-------------------------------------------------------+
c |                  Material Cards                       |
c +-------------------------------------------------------+
c m# isotope  percent   &(newline)    $comment
  m1   1000   1.0                        $Tr   .0001g/cc
c   m1  28063   1.0                      $63Ni    9.552 g/cc
  m2   8016    .3     7014   .7          $air     0.00129 g/cc
  m4  31000    .5     7000   .5          $GaN     6.15 g/cc
  m8  14000 .33  8000 .67                $SiO2    2.27 g/cc
  m9  13000 .4 8000 .6                   $Al2O3   3.98 g/cc
c +-------------------------------------------------------+
c |                  Source Definition                    |
c +-------------------------------------------------------+
sdef par=e  pos= 0 -0.00001 0 &
     erg=d4  axs=0 1 0 &
     rad=d1      ext=d3 &
     vec=0 1 0  dir=1
si1 0 .5  $radius of beam
 sp1 -21 1  $uniform distribution
si3 0 .00001       $linear distribution
sp3 -21 0       $probabilities
si4 0 .001 .0025 .0038 .005 .0063 .0076 .01 .013 .015 .016 .019
sp4 0 85   102   99    92   83    72    50  26   10   5    0       $3H

c +-------------------------------------------------------+
c |                  Data Cards                           |
c +-------------------------------------------------------+
mode p e                    $ n h d t s a these not needed
PHYS:P
PHYS:E
nps 24000000     $ .1Mh~.26min   90Mh~3hr
c +-------------------------------------------------------+
c |                  Tallies                              |
c +-------------------------------------------------------+
 fc14 flux averaged over the cell in particles/cm^2
  f14:e 3 4 5 6 7 8 9 10
  e14 0 38i .02
fc16 energy deposited averaged over cell MeV/g
 f16:p   3 4 5 6 7 8 9 10
 e16 0 38i .02
fc26  energy deposited averaged over cell MeV/g
 f26:e   3 4 5 6 7 8 9 10
 e26 0 38i .02
c
c +-------------------------------------------------------+
c |                  Mesh                                 |
c +-------------------------------------------------------+
c
 tmesh
c  flux=#/cm2     $dose=rem/hr    $pedep=MeV/cm3
  rmesh41:e  flux pedep dose
c depth profile
  cora41   -.6  58i   .6
  corb41   -.0002  98i  .0008
  corc41   -.6    .6
endmd
```

List of Symbols, Abbreviations, and Acronyms

2-D	two dimensional
C	diamond
CSDA	continuously slowing down approximation
DEC	direct energy conversion
EBIC	electron beam induced current
EHPs	electron-hole pairs
FOM	figure of merit
GaAs	gallium arsenide
GaN	gallium nitride
Ge	germanium
InP	indium phosphide
MCNPX	Monte Carlo n-particle extended
MOCVD	metallo-organic chemical vapor deposition
Ni	nickel
NIST	National Institute of Standards and Technology
Pm	promethium
Si	silicon
SiC	silicon carbide
SNR	signal-to-noise ratio
SUNY	State University of New York

1 DEFENSE TECHNICAL
(PDF) INFORMATION CTR
DTIC OCA

2 DIRECTOR
(PDFS) US ARMY RESEARCH LAB
RDRL CIO LL
IMAL HRA MAIL & RECORDS MGMT

1 GOVT PRINTG OFC
(PDF) A MALHOTRA

1 DIRECTOR
(PDF) US ARMY RESEARCH LAB
RDRL SER E
MARC LITZ

INTENTIONALLY LEFT BLANK.